On the Lifetime of Compressive Sensing Based Energy Harvesting in Underwater Sensor Networks

Huseyin Emre Erdem, Huseyin Ugur Yildiz, *Member, IEEE*, and Vehbi Cagri Gungor

***Abstract*—Recently, there has been a growing interest in academia and industry on the development of underwater acoustic sensor networks (UASNs) for scientific, commercial, and military purposes. Severe underwater channel conditions and limited battery energy of underwater nodes pose great challenges to prolong UASNs lifetime. Compressive sensing (CS), energy harvesting (EH), and transmission power control (TPC) are three promising solutions to improve UASNs lifetime. This paper aims to quantitatively investigate the joint impact of CS, EH, and TPC methods on the lifetime of UASNs. A novel Mixed Integer Programming (MIP) framework is developed to maximize the network lifetime by joint consideration of CS, EH, and TPC. Performance results show that the impact of CS on the network lifetime is higher than that of EH when both methods are combined with TPC. Moreover, when all three methods are combined, the network lifetime can be extended up to three times as compared to the case when all three methods are not utilized.**

***Index Terms*—compressive sensing, energy harvesting, network lifetime, optimization, underwater sensor networks.**

I. Introduction

UNDERWATER environment is yet to be fully exploited by industry and academia, since it poses many challenges to researchers and engineers. Limited bandwidth, impaired communication channel, high propagation delay, high bit error rate, and corrosive environment are among these hindrances [1]. Many underwater applications, such as pollution monitoring, seismic monitoring, and intruder detection use Underwater Acoustic Sensor Networks (UASNs) technology to periodically measure underwater environmental parameters over extended periods [2]. However, the network lifetime (*i.e.*, the duration when all the nodes are operational) is a critical limitation to meet underwater application requirements. The network lifetime depends on the amount of the available energy and the power consumption of underwater nodes.

Energy harvesting (EH) is an effective way to increase the amount of energy supplied to the sensor nodes by exploiting the ambient energy available in the environment [3]–[5]. The conversion from various forms of ambient energy into the electrical energy requires different devices specifically designed for each energy form. One of the most prominent resources to be exploited in the underwater environment is the *water currents*. The power that can be harvested from water currents is possible by using various types of mechanically or magnetically coupled devices, such as *hydrokinetic turbines* and *piezoelectric cantilevers* [6]. The underwater environment also possess ambient energy in acoustic form. This type of energy can be converted to electricity by using *hydrophones*.

Most of the energy is dissipated in the transceiver hardware of an underwater node. Excessive energy consumption of underwater nodes is caused by the transmission over long acoustic links and additional operations to compensate harsh channel conditions [7]. Therefore, decreasing the packet traffic in the network is mandatory for reducing the overall energy consumption. Compressive sensing (CS) is a promising solution for data compression such that CS theory states that a sparse signal (data) can effectively be sensed and reconstructed with fewer number of linear measurements (*i.e.*, the signal is directly sampled at lower than Nyquist rates [8]–[10]). Compared to the *regular sensing* where no compression is performed on the high-rate sampled data, CS introduces additional energy consumption during the data acquisition phase. The additional consumption is easily compensated by the energy cost reduction of packet transmissions, since the total number of packets to be transmitted is reduced in CS. The additional energy cost is smaller than that of data compression techniques when regular sensing is used. CS method requires the data to be sparse, *i.e.*, data to be sensed should contain small number of non-zero entries than zero entries in any domain such as frequency or wavelet. The ratio of the non-zero entries to the entire data size is called the *sparsity ratio*.

EH and CS methods have great potential to elongate the lifetime of UASNs. Furthermore, transmission power control (TPC) also helps in to attain the energy efficiency by assigning different transmission power levels at different transmission distances or channel conditions [11]. This way, significant amount of energy can be conserved as compared to the fixed transmission power strategy. Moreover, combining EH, CS, and TPC methods is expected to outperform these methods' individual impacts.

To the best of our knowledge, there is no controlled study in the literature that quantifies the impact of joint combination of EH, CS, and TPC methods on UASNs lifetime. The main contributions of this paper are enumerated as follows:

1) The impact of EH and CS methods on network lifetime is quantified by using different harvesters, namely *hydrokinetic turbine*, *piezoelectric cantilever*, and *hydrophone*. For a realistic assessment, an underwater energy consumption model utilizing TPC is developed.
2) A novel Mixed Integer Programming (MIP) framework is developed to determine the maximum network lifetime when EH, CS, and TPC are utilized together.

H. E. Erdem and V. C. Gungor are with the Department of Computer Engineering, Abdullah Gul University, Kayseri 38060, Turkey (e-mail: {huseyin.erdem,cagri.gungor}@agu.edu.tr)

H. U. Yildiz is with the Department of Electrical and Electronics Engineering, TED University, Ankara 06420, Turkey (e-mail: hugur.yildiz@tedu.edu.tr)

3) The impact of sensing distance and sparsity ratio on network lifetime is investigated using a target tracking scenario in an underwater environment.

The paper is structured as follows. Section II provides an overview of the current literature. Section III describes the underlying mechanics of this study. Section IV evaluates the findings using numerical results. Finally, Section V concludes the paper and provides future research directions.

II. Related Work

To date, there have been many studies that aim to present the benefits of EH and CS methods through analytical and experimental research in underwater environments. While some of these studies target energy neutral operation by adopting EH [12], others try to decrease energy consumption of the sensor nodes by using CS [13], [14].

In the underwater environment, *water currents* and *acoustic waves* are the main EH resources. There are some studies in the literature that use EH for underwater sensor nodes [15], [16]. However, these studies either do not provide a detailed analysis on the network lifetime or they focus solely on a single sensor node instead of a network. In [17] and [6], power consumptions of the nodes are assumed to be fixed without adopting any kind of TPC mechanisms. While [17] provides no information on the reporting rate which directly affects the overall power consumption of the nodes, [6] reports no detailed information on how the packets are relayed. [18] investigates only the power output of the harvester and does not present the impacts of this output on the node or network lifetime. Although [15] reports that the power output of their harvester manages to meet the requirements of the sensor node they choose, the reporting rate of a single daily measurement is not sufficient for most UASNs applications.

CS helps to decrease the number of packets to be transmitted in the network. However, CS requires the sensed data to be sparse. Only this way, CS can enable reduced data size while preserving the recoverability of the information to be forwarded. To analyze the impact of CS on the power consumption of sensor nodes, target tracking is usually to be the preferred scenario. Recently, CS based channel estimation methods have been proposed for sparse underwater channels. CS based methods can outperform subspace algorithms and least-squares based approaches in terms of block error rate [19]. Some studies eliminate the requirement of channel estimation by adopting a random access scheme. In [14], the randomness of CS measurements is exploited to be combined in a random Medium Access Control (MAC) scheme. In a random access MAC scheme, some packets may be dropped due to collisions. However, the dropped packets do not cause problems in a CS scenario, since it does not change the randomness of the data in the successfully transmitted packets. In order to guarantee the sufficient number of packets for successful reconstruction, increasing the number of nodes that sample the environment is sufficient. However, that study uses fixed transmission powers for all the nodes in the network. A simple packet drop rate is utilized instead of a realistic channel model (RCM).

TABLE I: Literature overview

Existing Studies	CS	EH	RCM	TPC
[13], [14]	✓	✗	✓	✗
[15], [16]	✗	✓	✗	✗
[17]	✗	✓	✗	✗
[6]	✗	✓	✗	✗
[18]	✗	✓	✗	✗
[19]	✓	✗	✓	✗
[20]	✗	✓	✓	✓
[21]	✓	✗	✓	✗
[22]	✓	✗	✓	✓
Our Work	✓	✓	✓	✓

In [21], CS and non-linear mapping are used together to decrease the data size and increase the transmission reliability of the packets. Wang *et al.* [22] focus on the aggregation of the data gathered from clustered nodes exploiting spatial and temporal correlations with CS. The data initially collected at cluster heads is sent to the sink node via multi-hop links. The authors state that the proposed solution can reduce the energy cost by more than 95% as compared to the conventional data aggregation schemes if the cluster number is 20. Jing *et al.* [20] propose a novel energy management algorithm to maximize the throughput of a node which is supplied with only limited power from an energy harvester. In that study, energy costs of data acquisition and transmission should be smaller than energy that the harvester is capable to provide in a single slot. At various harvesting rates, the energy allocation ratios for acquisition and transmission are decided using a dynamic programming approach.

An overview of the existing studies for the underwater networks mentioned above are listed in Table I. Although there are few studies that combine CS and EH for various scenarios (*e.g.*, [23], [24]), these studies only target terrestrial Wireless Sensor Networks (WSNs) instead of UASNs. To the best of our knowledge, there is no existing study that analyzes the lifetime of UASNs when both CS and EH are jointly adopted. To fill this gap in the literature, this study aims to present both the individual and joint impact of CS and EH methods on the lifetime of UASNs by adopting a target tracking scenario.

III. System Model

The scenario adopted in this study comprises of a mobile target traversing through an underwater region that is monitored by an underwater acoustic sensor network. The tracking of the vehicle is performed by using sensor measurements at consecutive rounds. The duration of each round is assumed to be pre-defined and sensor nodes may perform only a single measurement in each round. Only nodes with a distance to the target shorter than the sensing range can perform measurements. To evaluate the impact of CS on network lifetime, the measurements are made by using with or without CS. The sampling method directly affects the computation energy consumption and the amount of the generated packets. The generated packets are conveyed to the sink node using multi-hop routes. On the other hand, to evaluate the impact of EH on network lifetime, all the nodes are assumed to perform energy harvesting while they are in *idle* mode (*i.e.*, nodes either not sending or receiving packets).

A. Network Model

We adopt the network topology presented in [25] such that $N_{node} = 66$ sensor nodes are uniformly distributed within a rectangular area of $l_x \times l_y$ m^2. We have a single center-top positioned sink node. The depth of the network is l_z m. The 3D static network architecture is depicted in Fig. 1.

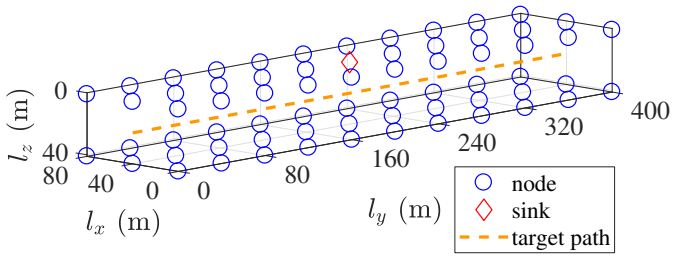

Fig. 1: Network architecture showing sink and node positions.

The target vehicle follows a linear path along the network (red dashed line in Fig. 1). The target is assumed to have a constant speed (υ_T knots). A single passage of the target may take several rounds, $N_{round} = l_y/(\tau_{rnd} \times \upsilon_T)$, where τ_{rnd} is the round duration. In each round, each node takes a single measurement if the target is within the pre-defined sensing distance (d_{sens}). The trigger is assumed be generated by comparing environmental acoustic noise levels to a pre-defined threshold. The power consumption of this additional operation (P_{sens}) is included in performance evaluations. The generated packets with payload size (M_P bytes) are sent to the sink node either directly or using multi-hop routes. Each generated packet has a header of size M_H bytes. The transmission time a single packet is represented by $\tau_{slot} = 8 \times M_P/R_b$ where R_b is the bit rate of the underwater sensor node. The duration of a single round is set to allow transmission of N_{max} many packets (*i.e.*, $\tau_{rnd} = N_{max} \times \tau_{slot}$). The total traffic of each node never surpasses the N_{max} value. Thus, each node has a sufficient time to transmit and receive its packets. Throughout the study, the number of passages until the first node depletes its energy is the preferred definition of the network lifetime. An example timing overview is provided in Fig. 2.

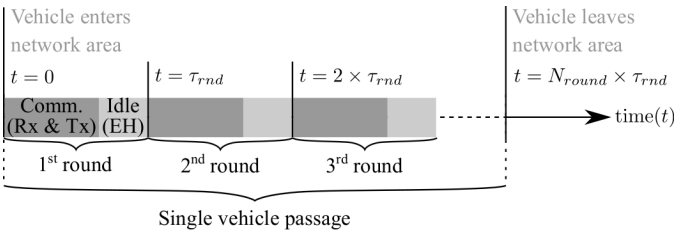

Fig. 2: Timing overview.

B. Sensing & Data Models

In the network, each sensor is attached with a camera that generates $87 \times 143 \times 3 = 36.4$ kilobytes of raw image data (*i.e.*, N) [26]. In this study, two different sensing models with and without CS are utilized. The first model is called "Regular Sensing (RS)" which performs sampling without CS with no further additional processing. The second model is called "CS" where the sparsity of the data is exploited to enable the recovery of the signal using fewer random samples [27]. Note that, sparse signals contain only a few non-zero coefficients and the signal in this study is assumed to be sparse in the frequency domain. Hence, the raw image data is assumed to be K-sparse (*i.e.*, K bytes of N bytes have non-zero entries)

The computational energy cost of RS comprises only the data acquisition energy (E_{ACQ}). On the other hand, the computational energy cost when CS is used comprises the data acquisition energy (E_{ACQ}), the signal processing energy costs (E_{SP}), and the background energy dissipation for other operations (E_{BCK}) [28]. Computational energy costs for RS (*i.e.*, E_{CMP-RS}) and CS (*i.e.*, E_{CMP-CS}) are defined as [28]

$$E_{CMP-RS} = E_{ACQ}, \tag{1}$$

$$E_{CMP-CS} = E_{ACQ} + E_{BCK} + E_{SP}. \tag{2}$$

Furthermore, the data acquisition energy is calculated as [28]

$$E_{ACQ} = N \times P_{ACQ} \times D_{OP}. \tag{3}$$

In Eq. (3), P_{ACQ}, and D_{OP} represent the data acquisition power (in Watts) and the instruction execution duration (in seconds), respectively. E_{BCK} and E_{SP} are calculated as [28]

$$E_{BCK} = P_{BCK} \times D_{SP}, \tag{4}$$

$$E_{SP} = N \times \epsilon_{mrd} + M \times N \times \epsilon_{add} + M \times \epsilon_{mwr}. \tag{5}$$

In Eq. (4), P_{BCK} and D_{SP} refer to the background power consumption and the execution duration for signal processing, respectively [28]. On the other hand, in Eq. (5), ϵ_{mrd}, ϵ_{add}, and ϵ_{mwr} represent energy dissipation values for reading from memory, addition, and writing to memory operations [28]. The total number of compressed measurements (M) is calculated by using the common assumption, $M = 4K$ [28].

C. Target Detection Model

In each round, each sensor node performs a single measurement only if the target vehicle is within a pre-defined sensing distance (*i.e.*, $d_{iT} \leq d_{sens}$) where d_{iT} is the distance between node-i and the target vehicle. Hence, the amount of data generated by each sensor node-i at each round-r for both RS and CS is calculated as

$$s_i^r = \begin{cases} \left\lceil \frac{N}{M_P - M_H} \right\rceil & \text{if } d_{iT} \leq d_{sens} \text{ for RS} \\ \left\lceil \frac{M}{M_P - M_H} \right\rceil & \text{if } d_{iT} \leq d_{sens} \text{ for CS} \\ 0 & \text{o.w.} \end{cases}, \forall i \in \mathcal{W}, r \in \mathcal{R}, \tag{6}$$

where $\mathcal{W}$ is the set of all sensor nodes and $\mathcal{R}$ represents the set of all rounds between 1 and N_{round}.

D. Target State Model

The target is assumed to follow a linear path that goes through the network volume along its y-axis as shown with red dashed line in Fig. 1. The state of the target vehicle is updated by using

$$X_{k+1} = \Phi X_k, \tag{7}$$

where, X_k and Φ represent the vehicle state at time instant-k and the state transition matrix [29]. X_k and Φ are calculated as

$$X_k = \begin{bmatrix} x_k & \dot{x}_k & y_k & \dot{y}_k & z_k & \dot{z}_k \end{bmatrix}^T, \tag{8}$$

$$\Phi = \begin{bmatrix} 1 & \tau_{rnd} & 0 & 0 & 0 & 0 \\ 0 & 1 & 0 & 0 & 0 & 0 \\ 0 & 0 & 1 & \tau_{rnd} & 0 & 0 \\ 0 & 0 & 0 & 1 & 0 & 0 \\ 0 & 0 & 0 & 0 & 1 & \tau_{rnd} \\ 0 & 0 & 0 & 0 & 0 & 1 \end{bmatrix}. \tag{9}$$

E. Physical Layer Model

In UASNs, the transmission power that is used for each node is determined based on the distance between the source node and the destination node while the reception power (P_{rx}) stays the same for all the nodes [30]. The electrical transmission power (P_{ij}^{tx}) that is used by node-i for transmission to node-j is calculated based on the required intensity at 1 meters of distance (I_{ij}^t) to the transmitter node which can be expressed as [31]

$$P_{ij}^{tx} = I_{ij}^t \times 2\pi \times 1m \times h_i, \tag{10}$$

where h_i is the depth of the transmitter node (in meters). On the other hand, I_{ij}^t is directly related to sound source level (*i.e.*, $\overline{SL_{ij}}$) in dB which is calculated as [31]

$$I_{ij}^t = 10^{\frac{\overline{SL_{ij}}}{10}} \times I_0, \tag{11}$$

where the reference intensity (*i.e.*, I_0) has the value of 0.67×10^{-18}. The sound source level is defined as

$$\overline{SL_{ij}} = \overline{A_{ij}} + \overline{\mathcal{N}} + \overline{\gamma_{ij}}, \tag{12}$$

where $\overline{A_{ij}}$, $\overline{\mathcal{N}}$ and $\overline{\gamma_{ij}}$ represent the path loss over link-(i,j), the ambient noise level, and the signal-to-noise ratio (SNR), respectively. Note that, we use overbars to represent each quantity in dB.

The path loss observed over link-(i,j) is effected by the transmission distance between node-i and node-j (*i.e.*, d_{ij}) and the operating frequency (f). The path loss over link-(i,j) is expressed as [25]

$$\overline{A_{ij}} = 10\kappa \log_{10}(d_{ij}) + \overline{\alpha(f)} \times d_{ij} \times 10^{-3}, \tag{13}$$

where κ represents spreading factor and $\overline{\alpha(f)}$ represents the absorption coefficient which is calculated as [30]

$$\overline{\alpha(f)} = \frac{0.11f^2}{1+f^2} + \frac{44f^2}{4100+f^2} + 2.75 \cdot 10^{-4} f^2 + 0.003. \tag{14}$$

The ambient noise level is the sum of noise levels caused by water turbulence (*i.e.*, $N_t(f)$), ships (*i.e.*, $N_s(f)$), thermal activities (*i.e.*, $N_{th}(f)$), and waves (*i.e.*, $N_w(f)$). The ambient noise level is defined as [25]

$$\overline{\mathcal{N}} = \overline{\mathcal{N}_t(f)} + \overline{\mathcal{N}_s(f)} + \overline{\mathcal{N}_{th}(f)} + \overline{\mathcal{N}_w(f)}. \tag{15}$$

We adopt the calculations of $\overline{\mathcal{N}_t(f)}$, $\overline{\mathcal{N}_s(f)}$, $\overline{\mathcal{N}_{th}(f)}$, and $\overline{\mathcal{N}_w(f)}$ derived in [25]. The bit error rate (BER) for 16-QAM modulation with Orthogonal Frequency Division Multiplexing (OFDM) transmission (which is adopted in this study from [31]) is expressed as

$$p_{ij}^b = \frac{3}{8}\text{erfc}\left(\sqrt{\frac{4}{10}\frac{B_N}{R_b}\gamma_{ij}}\right), \tag{16}$$

where B_N is the noise bandwidth (in Hz) and γ_{ij} is the SNR in the ordinary form. We adjust P_{ij}^{tx} values for each link to satisfy a certain BER performance (*i.e.*, $p_{ij}^b = 10^{-10}$).

F. Harvester Models

This part details the mathematical equations used to calculate power outputs of various energy harvesters.

1) Turbine Harvester: Turbine harvesters are utilized to convert the kinetic energy of a fluid flow into the electrical energy. The total amount of power available in a stream (P_{harv}) depends on the fluid density (ρ), wing spanning area (A), and flow speed (υ_f) [32]. P_{harv} is calculated as

$$P_{harv} = \frac{1}{2}\rho A {\upsilon_f}^3. \tag{17}$$

Note that $A = \pi r_d^2$ where r_d is the wing radius. The harvester cannot convert all the available energy into the electricity. Thus, the power value is multiplied with an efficiency coefficient (η_t). We adopt the υ_f values presented in [33].

2) Piezoelectric Harvester: Similar to the turbine harvester, the piezoelectric harvester aims to convert the ambient energy available in fluid flow into the electrical energy. In this type of harvester, uniformity of the flow should be disturbed to create vortexes that would help the piezoelectric cantilever to fluctuate and generate the electricity. The power output of the piezoelectric harvester (P_{harv}) is calculated as [34]

$$P_{harv} = 2f_v \left(W_{el\_cw} + W_{el\_ccw}\right), \tag{18}$$

where f_v represents vortex frequency; W_{el_cw} and W_{el_ccw} represent the electrical energy in clockwise and counter-clockwise directions, respectively. The vortex frequency is calculated by using the Strouhal Number (St) and the bluff size (D) as [34]

$$f_v = \frac{St \times \upsilon_f}{D}. \tag{19}$$

The electrical energy is calculated based on the cantilever specifications and the pressure difference as [34]

$$W_{el} = \frac{1}{128}\varrho^2 \frac{{d_{31}^p}^2}{\varepsilon_0 \varepsilon_r} \frac{BL^5}{{T_{pzt}}^3}. \tag{20}$$

where d_{31}^p, ε_0, and ε_r represent the piezoelectric constant, the absolute permittivity, and the relative permittivity, respectively. Moreover, B, $L = 2.1D$, and T_{pzt} define the cantilever width, length, and thickness, respectively. The pressure difference (ϱ) in clockwise and counter-clockwise directions are calculated as [34]

$$\varrho_{cw} = \frac{\rho}{2}{\upsilon_f}^2, \tag{21}$$

$$\varrho_{ccw} = -\frac{3}{2}\rho {\upsilon_f}^2. \tag{22}$$

Minimize E (26)

subject to:

$$\sum_{(i,j)\in\mathcal{A}} g_{ij}^r - \sum_{(j,i)\in\mathcal{A}} g_{ji}^r = \begin{cases} s_i^r & i \in \mathcal{W} \\ -\sum_{k\in\mathcal{W}} s_k^r & i = 1 \end{cases} \quad (27)$$
$$, \forall i \in \mathcal{V}, r \in \mathcal{R}$$

$$g_{1j}^r = 0, \forall j \in \mathcal{W}, r \in \mathcal{R} \quad (28)$$

$$g_{ij}^r \geq 0, \forall (i,j) \in \mathcal{A}, r \in \mathcal{R} \quad (29)$$

$$\sum_{r\in\mathcal{R}} \sum_{(i,j)\in\mathcal{A}} E_{tx,ij}^r + \sum_{r\in\mathcal{R}} \sum_{(j,i)\in\mathcal{A}} E_{rx,ji}^r + \sum_{r\in\mathcal{R}} E_{CMP} + \sum_{r\in\mathcal{R}} P_{sens} \times \tau_{i,sens}^r - \sum_{r\in\mathcal{R}} P_{harv,i} \times \tau_{i,idle}^r \leq E, \forall i \in \mathcal{W} \quad (30)$$

Fig. 3: The MIP framework that minimizes energy consumption of the most energy hungry node.

3) Hydrophone Harvester: Hydrophones are used to convert the energy of acoustic sound waves into the electrical energy. However, most of the time, the output of the hydrophone is not sufficient to be used in a scientific analysis. Thus, amplifiers are used to increase the signal gain. Nonetheless, amplifiers are active devices and they require power to operate. In this study, we are evaluating if the output of the hydrophone would produce enough power to have an impact on the network lifetime. The output power of a hydrophone (P_{harv}) can be calculated as [17]

$$P_{harv} = \eta_h \frac{10^{\frac{\overline{RL_{ij}} + \overline{RVS}}{10}}}{4R_p}, \quad (23)$$

where $\overline{RL_{ij}} = \overline{SL_{ij}} - \overline{A_{ij}}$ represents the received signal level in dB. η_h, $\overline{RVS}$, and R_p are the hydrophone efficiency (in percentage), the voltage sensitivity, and the load impedance, respectively.

The total acoustic energy available in a single ship passage (which has a speed of v_{ship} taking a distance of l_{max}) is expressed as

$$E_{ship} = \int_{t=0}^{\frac{l_{max}}{v_{ship}}} P_{harv}(t) \mathrm{d}t. \quad (24)$$

Given n_{ship} number of ship passages in a single day on the average, the daily average harvested power for a 5-hydrophone harvester setup is calculated as

$$P_{daily,harv} = 5 \frac{E_{ship} \times n_{ship}}{24 \times 60 \times 60}. \quad (25)$$

G. The MIP Model for Energy Minimization

In Fig. 3, we present the MIP framework which determines the best packet routes that minimizes the energy consumption of the most energy hungry node (E). The objective function of the MIP framework is to minimize E which is defined in (26). The MIP model is subject to constraints presented in (27)–(30).

In this study, the network is represented as a directed graph of $G(\mathcal{V}, \mathcal{A})$ where $\mathcal{V}$ and $\mathcal{A}$ represent the set of all the nodes (including the central sink node) and the set of all the directed links between all node pairs, respectively. Moreover, we define $\mathcal{W}$ to represent the set of all the nodes except the sink node (*i.e.*, node-1). As stated previously, $\mathcal{R}$ represents the set of all rounds between 1 and N_{round}.

The decision variable of the MIP model is the number of flows transmitted from node-i to node-j in the r^{th} round which is represented by the integer variable, g_{ij}^r. The decision of flows is made based on the constraints of the MIP framework as well as the parameters. The first parameter is the number of generated data packets (s_i^r) by node i in the r^{th} round which has already been defined in Eq. (6). Another parameter is the computational energy cost of a single node (E_{CMP}) which is defined in Eq. (1) for RS and Eq. (2) for CS. The power consumption of each node to sense the presence of a passing vehicle is denoted as P_{sens} parameter. Finally, $P_{harv,i}$ values are determined in Eqs. (17), (18), and (25) for the turbine, the piezoelectric, and the hydrophone harvesters, respectively.

Const. (27) guarantees that for each node except the sink node, the amount of generated data packets is equal to the difference between the transmitted packets and the received packets. For the sink node, this constraint forces the same difference to be equal to the total number of packets generated by all the other nodes. Consts. (28) and (29) state that the sink node cannot generate packets and the flow values cannot be negative, respectively. Const. (30) obligates that the sum of the net energy consumption (*i.e.*, consumed energy – harvested energy) of each node (except the sink) in each round has to be smaller than or equal to the objective. It is important to note that the total energy consumption of a node is the sum of energy costs for packet transmissions, packet receptions, computational operations, and sensing operations.

Energy costs for packet transmissions and receptions in each round-r are denoted by $E_{tx,ij}^r$ and $E_{rx,ij}^r$, respectively. $E_{tx,ij}^r$ and $E_{rx,ij}^r$ are calculated as

$$E_{tx,ij}^r = P_{ij}^{tx} \times \tau_{slot} \times g_{ij}^r, \ \forall (i,j) \in \mathcal{A}, r \in \mathcal{R}, \quad (31)$$

$$E_{ij}^{r,rx} = P_{rx} \times \tau_{slot} \times g_{ji}^r, \ \forall (i,j) \in \mathcal{A}, r \in \mathcal{R}. \quad (32)$$

To calculate the energy consumption and generation levels of sensing and harvesting operations, the duration of each of these operations should be known. This study assumes that the sensing is performed when the node does not make any transmissions. Similarly, harvesting is performed when the node is in the idle mode. According to this information, the sensing duration and the idle time duration are denoted by $\tau_{i,sens}^r$ and $\tau_{i,idle}^r$ which are calculated as

$$\tau_{i,sens}^r = \tau_{rnd} - \tau_{slot} \times \sum_{(i,j)\in\mathcal{A}} g_{ij}^r, \ \forall i \in \mathcal{W}, r \in \mathcal{R}, \quad (33)$$

$$\tau^r_{i,idle} = \tau_{rnd} - \tau_{slot} \times \left(\sum_{(i,j)\in\mathcal{A}} g^r_{ij} + \sum_{(j,i)\in\mathcal{A}} g^r_{ji} \right), \ \forall i \in \mathcal{W}, \ \forall r \in \mathcal{R}. \quad (34)$$

IV. Performance Analysis

In this section, the joint impact of EH and CS on network lifetime is investigated. We use General Algebraic Modeling System (GAMS) with CPLEX solver [35] to optimize packet routes where we minimize the energy consumption of the most energy hungry node based on node residual energies. GAMS is a high-level optimization tool that consists of a language compiler and high-performance solvers. We use the CPLEX solver which uses branch and cut method to solve the MIP framework to optimality. CPLEX solver is chosen since it can solve large and difficult problems in an efficient manner with minimal user intervention. For problems with integer variables, as we have in this work, CPLEX solver uses branch and cut method which solves a series of subproblems of linear programming types to solve the original problem. CPLEX has the advantage of choosing the best solver options for a given MIP problem.

The simulation parameters are listed in Table II. In our simulations, we use the network topology presented in Fig. 1 such that the sensing distance (d_{sens}) is varied between 40 m and 320 m. Moreover, we choose four sparsity ratios (K/N) which are 0.08, 0.12, 0.16, and 0.20.

In Fig. 4a, we present the energy consumption of the most energy hungry node for the three type of harvesters. Our results reveal that the turbine harvester provides the most harvested energy among all three types of harvesters which is followed by the piezoelectric harvester and the hydrophone harvester. The hydrophone harvester provides insignificant amount of energy to the sensor nodes.

We illustrate the impact of using the three energy harvesters on network lifetime in Fig. 5a. The *y*-axis of this figure shows the lifetime improvements which are calculated by determining the percent increment between the network lifetime that is obtained when an EH device is used and the network lifetime that is obtained when an EH device is not used. As seen from this figure, the turbine harvester can provide up to 30% improved network lifetimes. Nonetheless, the piezoelectric harvester yields at most 10% prolonged network lifetimes. As stated previously, the hydrophone harvester cannot provide significant improvements in network lifetimes. The major trend of the impacts in Figs. 4a and 5a is inversely proportional to the sensing distance. As d_{sens} increases, more nodes generate packets which are conveyed to the sink node. As a result, nodes closer to the sink node have more packets to relay thus increasing the overall energy consumption in the network. Lifetime improvements are up to 9% when d_{sens} increases.

In Figs. 4b and 5b, impacts of individual and joint utilization of CS and EH are depicted. The sparsity ratio is fixed to 0.16 and results are provided as a function of d_{sens}. In the remaining figures (*i.e.*, Figs. 4b, 4c, 5b, and 5c), EH refers to the turbine harvester since it is the preferred energy harvester due to its high output. The benchmark curves which are labeled as "None" in Figs. 4b and 4c show the results without using CS and EH. Our analysis shows that CS provides better lifetimes than EH if they are used individually. However, the lifetime improvement of EH is inversely proportional to d_{sens}. For example, when $d_{sens} = 40$ m, EH improves network lifetimes by 30%. However, EH can improve the network lifetime only by 9% when d_{sens} is increased to 160 m. When d_{sens} is high, more nodes are involved in packet generation which eventually increases the overall energy consumption. Since CS helps to decrease the amount of packets to be traversed in the network, this solution provides better network lifetimes than EH when d_{sens} is high. Lifetime improvements are greater than 100% if both methods are combined (*viz.*, EH & CS curve).

In Figs. 4c and 5c, we fix $d_{sens} = 160$ m and vary the sparsity ratio. EH is not effected by the sparsity ratio where this method provides 13% prolonged network lifetimes. For low K/N values, CS has the superior advantage such that network lifetimes can be improved up to 170%. Moreover, the lifetime improvement surpasses 300% when CS and EH

TABLE II: Simulation Parameters

Network Parameters		
N_{node}	Number of nodes	66
l_x	Network width (m)	80
l_y	Network length (m)	400
l_z	Network height (m)	40
l_{grid}	Network grid length (m)	40
v_T	Target speed (knots)	1
N_{max}	Maximum number of packets in a single round	200
Modem & Channel Parameters		
R_b	Data rate (kbps)	5
P_{rx}	Reception power (W)	3
P_{sens}	Sensing power (mW)	5.7
f	Frequency (kHz)	25
p^b_{ij}	Bit error rate on link-(i,j)	10^{-10}
N	Raw data size (KB)	36.4
M_P	Payload size (bytes)	1000
M_H	Header size (bytes)	20
K/N	Sparsity ratio	0.08–0.20
d_{sens}	Sensing distance (m)	40–320
κ	Spreading factor	1.5
B_N	Noise bandwidth (kHz)	1
Turbine Harvester Parameters		
r_d	Wing radius (m)	0.025
η_t	Turbine efficiency (%)	6
ρ	Density of ocean water (kg/m^3)	1000
Piezoelectric Harvester Parameters		
L	Cantilever length (mm)	50
B	Cantilever width (mm)	3
ε_r	Relative permittivity	4000
ε_0	Absolute permittivity (F/m)	8.85×10^{-12}
T_{pzt}	Thickness (μm)	60
d^p_{31}	Piezoelectric constant (C/N)	300×10^{-12}
St	Strouhal number	0.2
Hydrophone Harvester Parameters		
$\overline{SL_{ij}}$	Sound source level (dB)	188.1
$\overline{RVS}$	Receiving voltage sensitivity (dB re $1V/\mu$Pa)	-186
R_p	Load impedance (ohms)	125
n_{ship}	Number of ships	2000
l_{max}	Distance taken by ships (m)	200
v_{ship}	Speed of ships (knots)	1
η_h	Efficiency of the hydrophone (%)	70

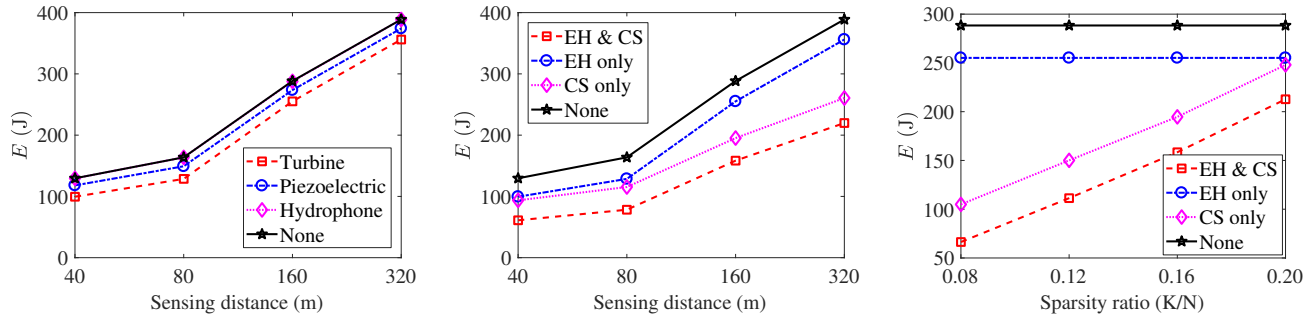

Fig. 4: The objective value (E – in J) for the three energy harvesters as a function of sensing distance (d_{sens}) when the sparsity ratio (K/N) is fixed to 0.16 (a); E values for the proposed approaches as a function of d_{sens} when $K/N = 0.16$ (b) and as a function of K/N when $d_{sens} = 160$ m (c).

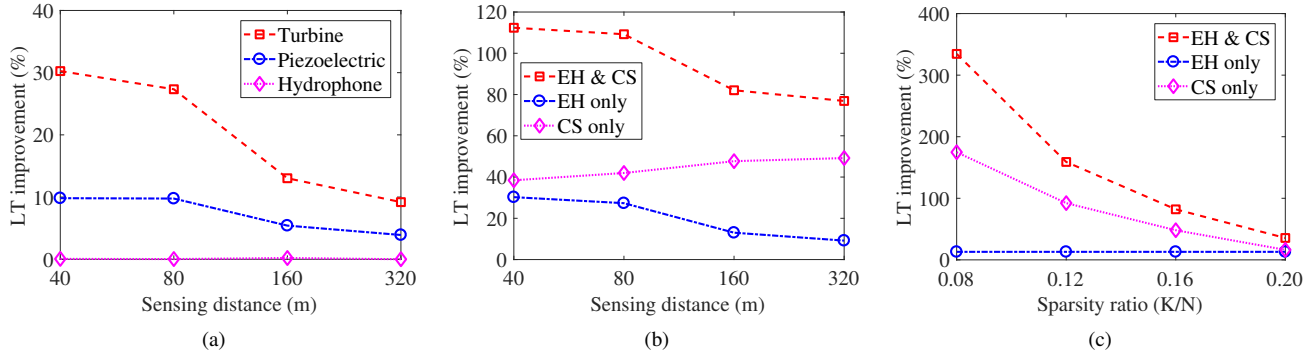

Fig. 5: Lifetime (LT) improvements for the three energy harvesters as a function of sensing distance (d_{sens}) when the sparsity ratio (K/N) is fixed to 0.16 (a); LT improvements for the proposed approaches as a function of d_{sens} when $K/N = 0.16$ (b) and as a function of sparsity ratio (K/N) when $d_{sens} = 160$ m (c).

are used together. On the other hand, when K/N increases, the advantage of utilizing CS diminishes. In this configuration, the number of packets that are generated greatly increases which would result in excessive energy consumption in the network. As a result, CS can provide at most 16% prolonged network lifetimes. Nevertheless, network lifetimes can be improved by 35% if both EH and CS are used together when $K/N = 0.20$.

V. Conclusion

This study aims to analyze the impacts of three EH methods (*i.e.*, turbine harvester, piezoelectric harvester, hydrophone harvester) as well as CS technique on network lifetimes. A novel MIP framework is developed to maximize the network lifetime which jointly considers CS, EH, and TPC methods by adopting a realistic channel model. The main conclusions drawn from this paper are enumerated as follows:

1) Increasing the sensing distance results in high number of generated packets which greatly increase the overall energy consumption in the network. For a fixed sparsity ratio, usage of CS rather than EH results in more extended lifetimes.
2) Considering the three harvester types, the turbine harvester outperforms other type of harvesters when used under the simulated conditions. The turbine harvester can provide at least 9%, at most 30% prolonged lifetimes as compared to the lifetimes obtained without EH. Similarly, the piezoelectric harvester extends the lifetimes by 4%–10%. Using the hydrophone harvester does not provide significant improvements in network lifetimes.
3) For a fixed sensing distance, CS can further prolong the network lifetime than EH especially when the sensed signal is sparse (*i.e.*, $K/N = 0.08$). Our results show that CS can extend the network lifetime up to 170% while EH improves the network lifetime up to 13% as compared to the lifetimes obtained without EH and CS. For non-sparse signals (*i.e.*, $K/N = 0.20$), CS loses its superiority against EH.
4) It is shown that joint utilization of EH and CS can improve the network lifetime up to 300% as compared to the lifetimes obtained without EH and CS.

Future work includes investigating the impact of node mobility and error control approaches for efficient packet delivery in UASNs. Extension of our framework by using ray tracing-based channel models (*e.g.*, BELLHOP) is also considered as a future work. Moreover, validation of the proposed solution through experimental evaluations for UASNs testbeds is an important future research since the there is no globally adopted underwater channel model in the research community.

ACKNOWLEDGEMENT

The work of H. E. Erdem and V. C. Gungor were supported by TUBITAK 1001 Project (project no: 114E248).

REFERENCES

[1] I. F. Akyildiz, D. Pompili, and T. Melodia, "Underwater acoustic sensor networks: research challenges," *Ad Hoc Netw.*, vol. 3, no. 3, pp. 257–279, 2005.

[2] F. Wu and K. Yang and R. Duan and T. Tian, "Compressive Sampling and Reconstruction of Acoustic Signal in Underwater Wireless Sensor Networks," *IEEE Sens. J.*, vol. 18, no. 14, pp. 5876–5884, 2018.

[3] A. Kansal, J. Hsu, S. Zahedi, and M. B. Srivastava, "Power management in energy harvesting sensor networks," *ACM T. Embed. Comput. S.*, vol. 6, no. 4, 2007, art. no. 32.

[4] L. Jing and C. He and J. Huang and Z. Ding, "Energy Management and Power Allocation for Underwater Acoustic Sensor Network," *IEEE Sens. J.*, vol. 17, no. 19, pp. 6451–6462, 2017.

[5] D. Zhang and M. Liu and S. Zhang and Q. Zhang, "Non-myopic energy allocation for target tracking in energy harvesting UWSNs," *IEEE Sens. J.*, vol. PP, pp. 1–1, 2019.

[6] F. U. Qureshi, A. Muhtaroğlu, and K. Tuncay, "Near-optimal design of scalable energy harvester for underwater pipeline monitoring applications with consideration of impact to pipeline performance," *IEEE Sens. J.*, vol. 17, no. 7, pp. 1981–1991, 2017.

[7] I. F. Akyildiz, D. Pompili, and T. Melodia, "State-of-the-art in protocol research for underwater acoustic sensor networks," in *Proc. ACM Int. Workshop on Underwater Netw. (WUWNet)*, 2006, pp. 7–16.

[8] R. G. Baraniuk, "Compressive sensing [lecture notes]," *IEEE Signal Proc. Mag.*, vol. 24, no. 4, pp. 118–121, 2007.

[9] E. J. Candes and M. B. Wakin, "An introduction to compressive sampling," *IEEE Signal Proc. Mag.*, vol. 25, no. 2, pp. 21–30, 2008.

[10] J. E. Barceló-Lladó and A. Morell and G. Seco-Granados, "Amplify-and-Forward Compressed Sensing as an Energy-Efficient Solution in Wireless Sensor Networks," *IEEE Sens. J.*, vol. 14, no. 5, pp. 1710–1719, 2014.

[11] H. U. Yildiz and B. Tavli and H. Yanikomeroglu, "Transmission Power Control for Link-Level Handshaking in Wireless Sensor Networks," *IEEE Sens. J.*, vol. 16, no. 2, pp. 561–576, 2016.

[12] P. Zhang, G. Xiao, and H.-P. Tan, "Clustering algorithms for maximizing the lifetime of wireless sensor networks with energy-harvesting sensors," *Comput. Netw.*, vol. 57, no. 14, pp. 2689–2704, 2013.

[13] F. Fazel, M. Fazel, and M. Stojanovic, "Random access compressed sensing for energy-efficient underwater sensor networks," *IEEE J. Sel. Area Comm.*, vol. 29, no. 8, pp. 1660–1670, 2011.

[14] ——, "Compressed sensing in random access networks with applications to underwater monitoring," *Phys. Commun.*, vol. 5, no. 2, pp. 148–160, 2012.

[15] H. F. Rezaei, A. Kruger, and C. Just, "An energy harvesting scheme for underwater sensor applications," in *Proc. IEEE Int. Conf. Electro/Inform. Technol.*, 2012, pp. 1–4.

[16] Y. Cha, H. Kim, and M. Porfiri, "Energy harvesting from underwater base excitation of a piezoelectric composite beam," *Smart Mater. Struct.*, vol. 22, no. 11, p. 115026, 2013.

[17] A. Bereketli and S. Bilgen, "Remotely powered underwater acoustic sensor networks," *IEEE Sens. J.*, vol. 12, no. 12, pp. 3467–3472, 2012.

[18] D. M. Toma, J. del Rio, M. Carbonell-Ventura, and J. M. Masalles, "Underwater energy harvesting system based on plucked-driven piezoelectrics," in *Proc. OCEANS 2015 - Genova*, 2015, pp. 1–5.

[19] C. R. Berger, S. Zhou, J. C. Preisig, and P. Willett, "Sparse channel estimation for multicarrier underwater acoustic communication: From subspace methods to compressed sensing," *IEEE T. Signal Proces.*, vol. 58, no. 3, pp. 1708–1721, 2010.

[20] L. Jing, C. He, J. Huang, and Z. Ding, "Energy management and power allocation for underwater acoustic sensor network," *IEEE Sens. J.*, vol. 17, no. 19, pp. 6451–6462, 2017.

[21] I. Iglesias, A. Song, J. Garcia-Frias, M. Badiey, and G. R. Arce, "Image transmission over the underwater acoustic channel via compressive sensing," in *Proc. Annnual Conf. Inform. Sci. Syst.*, 2011, pp. 1–6.

[22] D. Wang, R. Xu, X. Hu, and W. Su, "Energy-efficient distributed compressed sensing data aggregation for cluster-based underwater acoustic sensor networks," *Int. J. Distrib. Sens. N.*, vol. 12, no. 3, 2016, art. no. 8197606.

[23] R. Rana, W. Hu, and C. T. Chou, "Energy-aware sparse approximation technique (EAST) for rechargeable wireless sensor networks," in *Proc. Wirel. Sens. Netw.*, 2010, pp. 306–321.

[24] W. Chen, Y. Andreopoulos, I. J. Wassell, and M. R. D. Rodrigues, "Towards energy neutrality in energy harvesting wireless sensor networks: A case for distributed compressive sensing?" in *Proc. IEEE Global Commun. Conf. (GLOBECOM)*, 2013, pp. 474–479.

[25] A. Stefanov and M. Stojanovic, "Design and performance analysis of underwater acoustic networks," *IEEE J. Sel. Area Comm.*, vol. 29, no. 10, pp. 2012–2021, 2011.

[26] I. Vasilescu, K. Kotay, D. Rus, M. Dunbabin, and P. Corke, "Data collection, storage, and retrieval with an underwater sensor network," in *Proc. Int. Conf. Embed. Netw. Sens. Syst. (SenSys)*, 2005, pp. 154–165.

[27] D. L. Donoho, "Compressed sensing," *IEEE T. Inform. Theory*, vol. 52, no. 4, pp. 1289–1306, 2006.

[28] C. Karakus, A. C. Gurbuz, and B. Tavli, "Analysis of energy efficiency of compressive sensing in wireless sensor networks," *IEEE Sens. J.*, vol. 13, no. 5, pp. 1999–2008, 2013.

[29] Y. Petillot, I. T. Ruiz, and D. M. Lane, "Underwater vehicle obstacle avoidance and path planning using a multi-beam forward looking sonar," *IEEE J. Oceanic Eng.*, vol. 26, no. 2, pp. 240–251, 2001.

[30] J. M. Jornet, M. Stojanovic, and M. Zorzi, "On joint frequency and power allocation in a cross-layer protocol for underwater acoustic networks," *IEEE J. Oceanic Eng.*, vol. 35, no. 4, pp. 936–947, 2010.

[31] M. Felemban and E. Felemban, "Energy-delay tradeoffs for underwater acoustic sensor networks," in *Proc. Int. Black Sea Conf. Commun. and Netw. (BlackSeaCom)*, 2013, pp. 45–49.

[32] H. J. Vermaak, K. Kusakana, and S. P. Koko, "Status of micro-hydrokinetic river technology in rural applications: A review of literature," *Renew. Sust. Energ. Rev.*, vol. 29, pp. 625–633, 2014.

[33] E. Jarosz, W. J. Teague, J. W. Book, and k. Beşiktepe, "On flow variability in the Bosphorus strait," *J. Geophys. Res-Oceans*, vol. 116, no. C8.

[34] S. Pobering and N. Schwesinger, "A novel hydropower harvesting device," in *Proc. Int. Conf. MEMS, NANO and Smart Syst. (ICMENS)*, 2004, pp. 480–485.

[35] "CPLEX 12," Accessed: 4 December 2018. [Online]. Available: https://www.gams.com/latest/docs/S_CPLEX.html

Huseyin Emre Erdem received his B.S. degree in Mechatronics Engineering from Kocaeli University, Turkey in 2011 and his M.S. degree in Autonomous Robotics Engineering from University of York, UK in 2014. He is currently a PhD student in Electrical and Computer Engineering program at Abdullah Gul University (AGU), Turkey. His current research areas include Wireless Sensor Networks and Underwater Acoustic Networks.

Huseyin Ugur Yildiz (S'13-–M'16) received the B.S. degree from Bilkent University, Ankara, Turkey, in 2009; the M.S. and Ph.D. degrees from TOBB University of Economics and Technology, Ankara, Turkey, in 2013 and 2016, respectively, all in electrical and electronics engineering. He is an Assistant Professor in the Department of Electrical and Electronics Engineering at TED University, Ankara, Turkey. His research focuses on the applications of optimization techniques for modeling and analyzing research problems on wireless communications, wireless networks, underwater acoustic networks, and smart grids.

Vehbi Cagri Gungor received his B.S. and M.S. degrees in Electrical and Electronics Engineering from Middle East Technical University, Ankara, Turkey, in 2001 and 2003, respectively. He received his Ph.D. degree in electrical and computer engineering from the Broadband and Wireless Networking Laboratory, Georgia Institute of Technology, Atlanta, GA, USA, in 2007. Currently, he is a Full Professor and Chair of Computer Engineering Department, Abdullah Gul University (AGU), Kayseri, Turkey. His current research interests are in smart grid communications, machine-to-machine communications, next-generation wireless networks, wireless ad hoc and sensor networks, and cognitive radio networks.